

# Supporting Information: Equilibration of ion distribution at polymer/ceramic interface

Melania Kozdra<sup>1</sup>, Laura Hölzer<sup>2</sup>, Daniel Brandell<sup>1</sup>, and Andreas Heuer<sup>2</sup>

<sup>1</sup>Department of Chemistry - Ångström Laboratory, Uppsala University, Box 538, 75121 Uppsala, Sweden

<sup>2</sup>Institute of Physical Chemistry - University Muenster

## Flow Chart

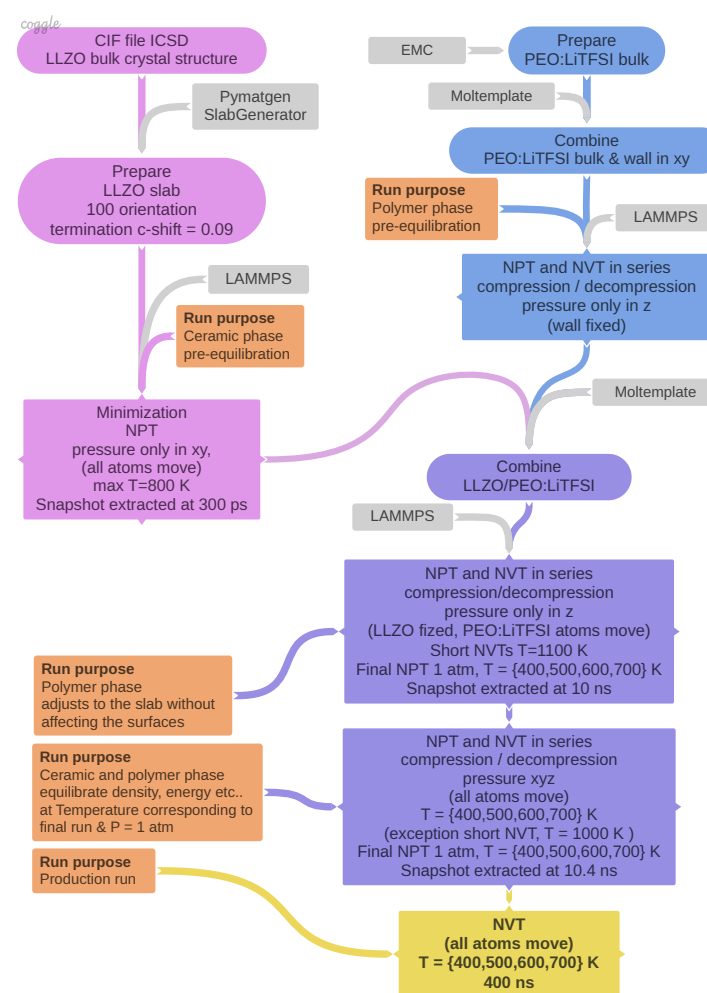


Figure S1: Flow chart describing the equilibration procedure from bulk ceramic and polymer phases to production runs of LLZO/PEO:LiTFSI interface.

## Additional table

Table S1: Bins msd  $z \in \{..\}$  Å

Li <sup>+</sup>	-55	-40	-32	-23	-15	-5	5	15	23	32	40	55
TFSI <sup>-</sup>	-55	-40	-32	-26	-19	-	-	19	26	32	40	55

## Additional figures

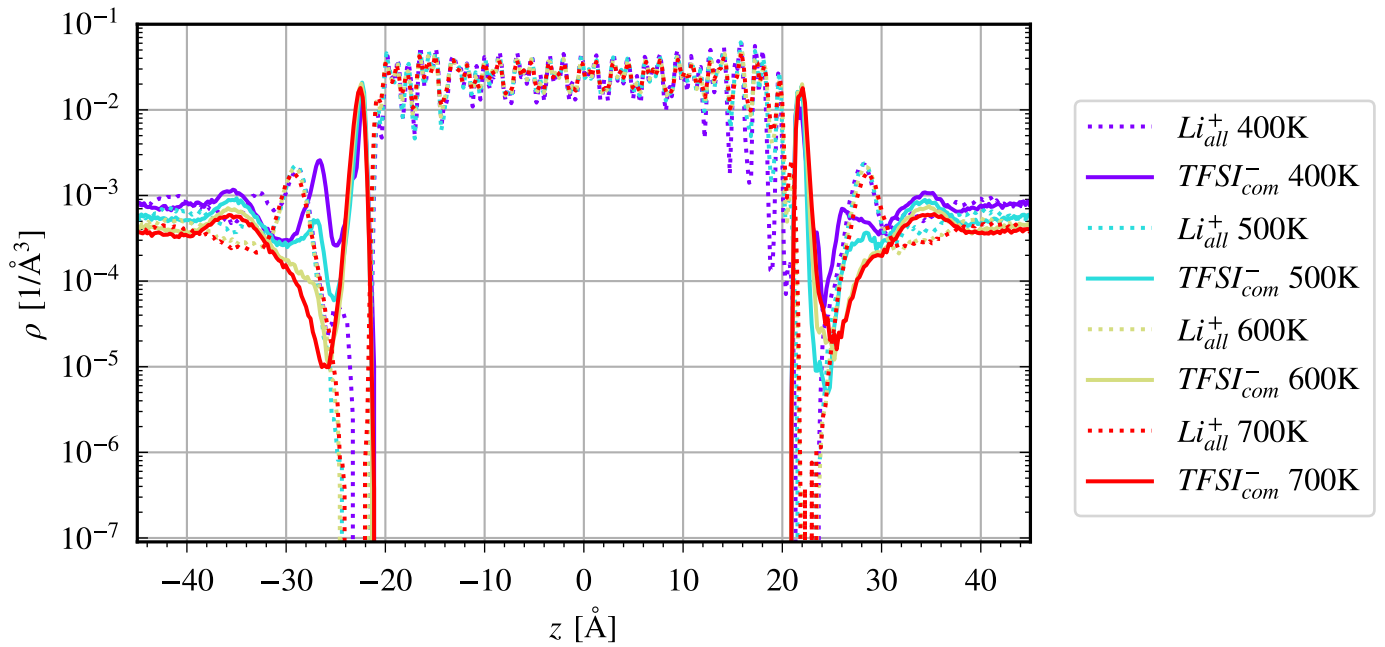


Figure S2: Mean atom density profile of Li<sup>+</sup> and TFSI<sup>-</sup> at different temperatures (400K, 500K, 600K and 700K).

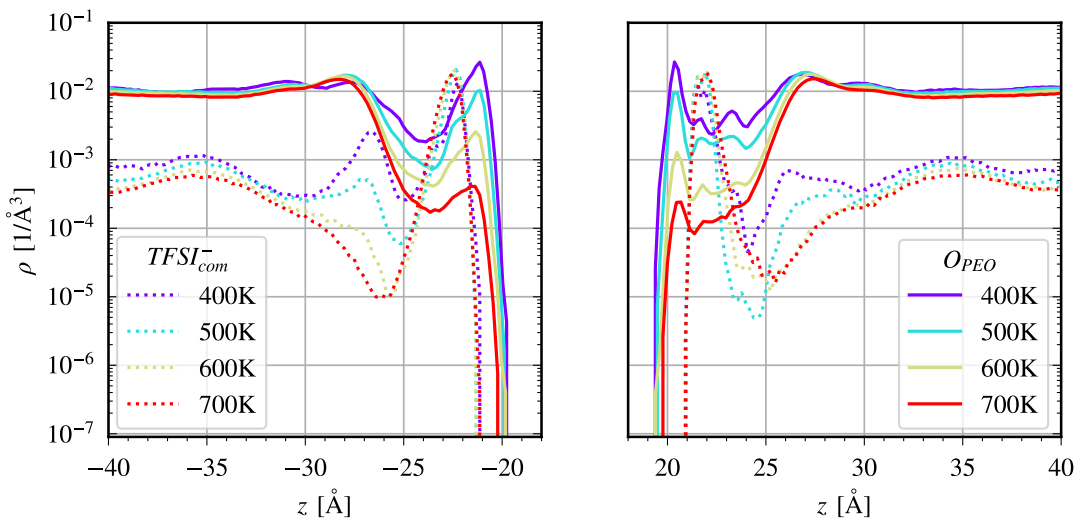


Figure S3: Mean atom density profile of TFSI<sup>-</sup> and OPEO at the LEFT and RIGHT interface of the LLZO slab at at different temperatures (400K, 500K, 600K and 700K).

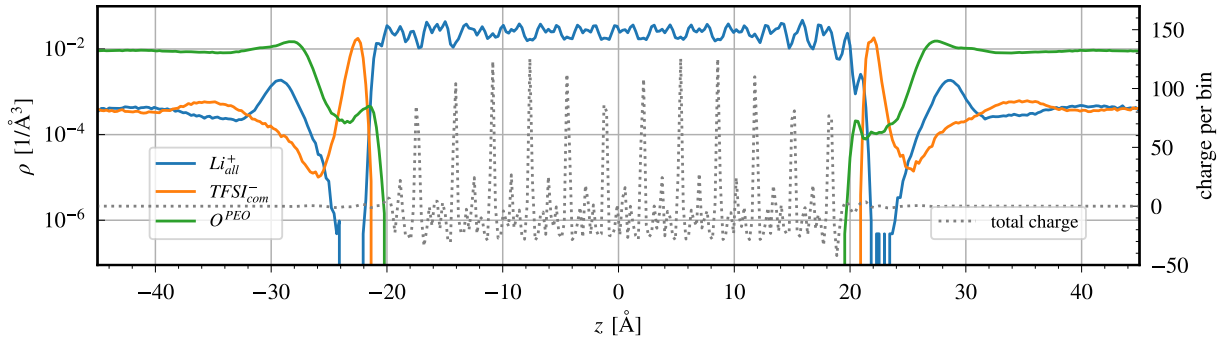


Figure S4: Mean atom density profile of  $\text{Li}^+$ ,  $\text{TFSI}^-$  and  $\text{O}^{\text{PEO}}$  at 700K and distribution of total charge.

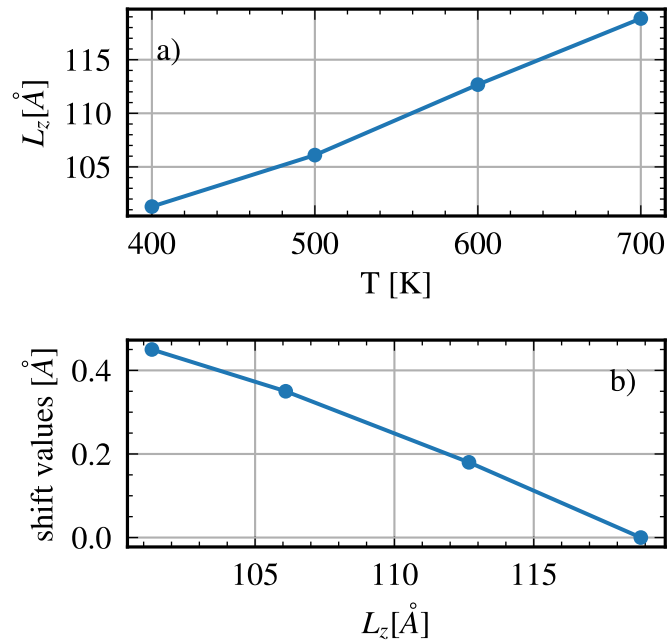


Figure S5: a ) Simulation box length, perpendicular to the LLZO surface  $L_z$ , in the final NVT run as a function of simulation temperature. b) Shift values as a function of  $L_z$  (see also figure S6).

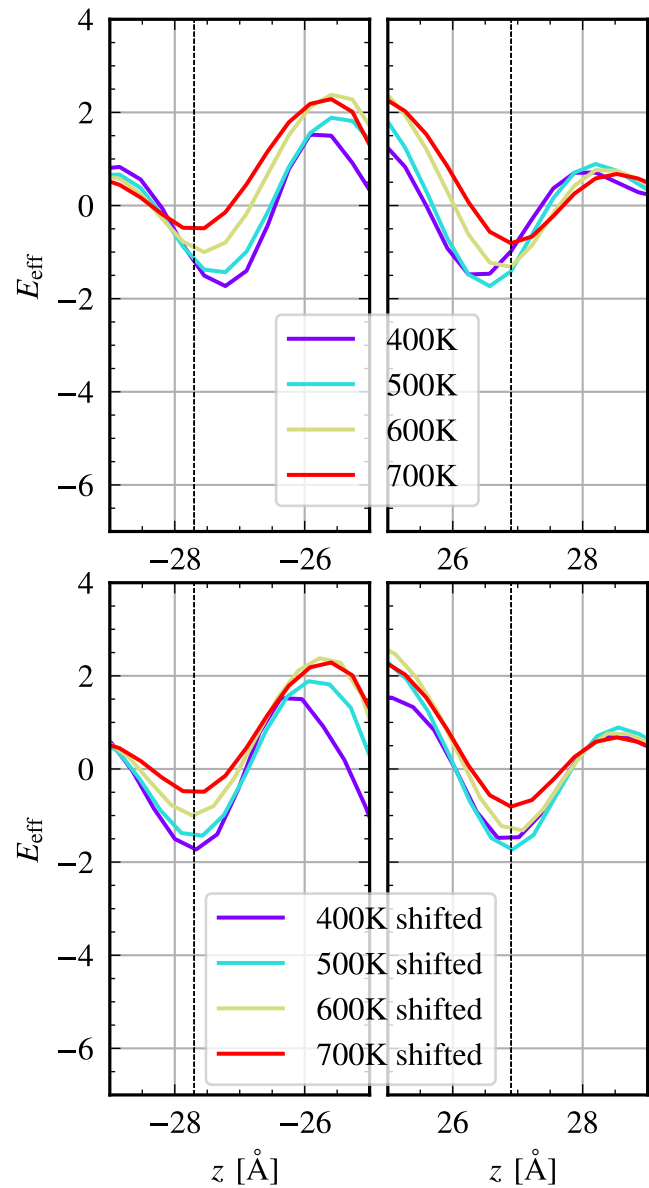


Figure S6: Integrated total charge around the LEFT and RIGHT LLZO-SPE interface for simulations at 400 K, 500 K, 600 K and 700 K. The second row is shifted (shift values in order of legend: [0.45, 0.35, 0.18, 0], - for LEFT, + for RIGHT side)

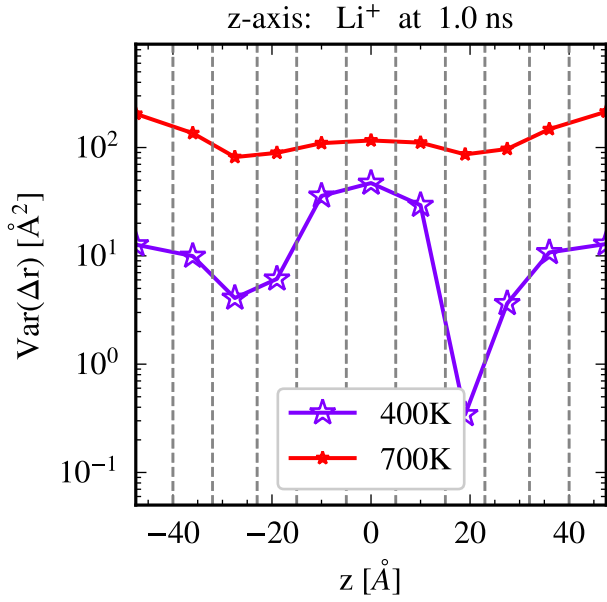


Figure S7: Displacement variance of  $\text{Li}^+$  at 1 ns in  $z$ -axis (perpendicular to LLZO surface) as a function of ions position perpendicular to the LLZO surface. The vertical gray dashed lines indicate the bins used for the calculation of specially resolved  $\text{Var}(\Delta r)$ . Last 300 ns of NVT trajectories at 400 and 700 K were taken for the analysis.

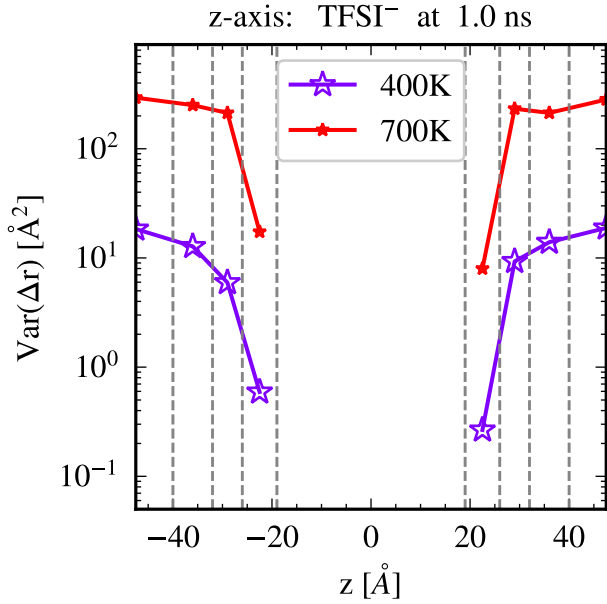


Figure S8: Displacement variance of  $\text{TFSI}^-$  at 1 ns in  $z$ -axis (perpendicular to LLZO surface) as a function of ions position perpendicular to the LLZO surface. The vertical gray dashed lines indicate the bins used for the calculation of specially resolved  $\text{Var}(\Delta r)$ . Last 300 ns of NVT trajectories at 400 and 700 K were taken for the analysis.

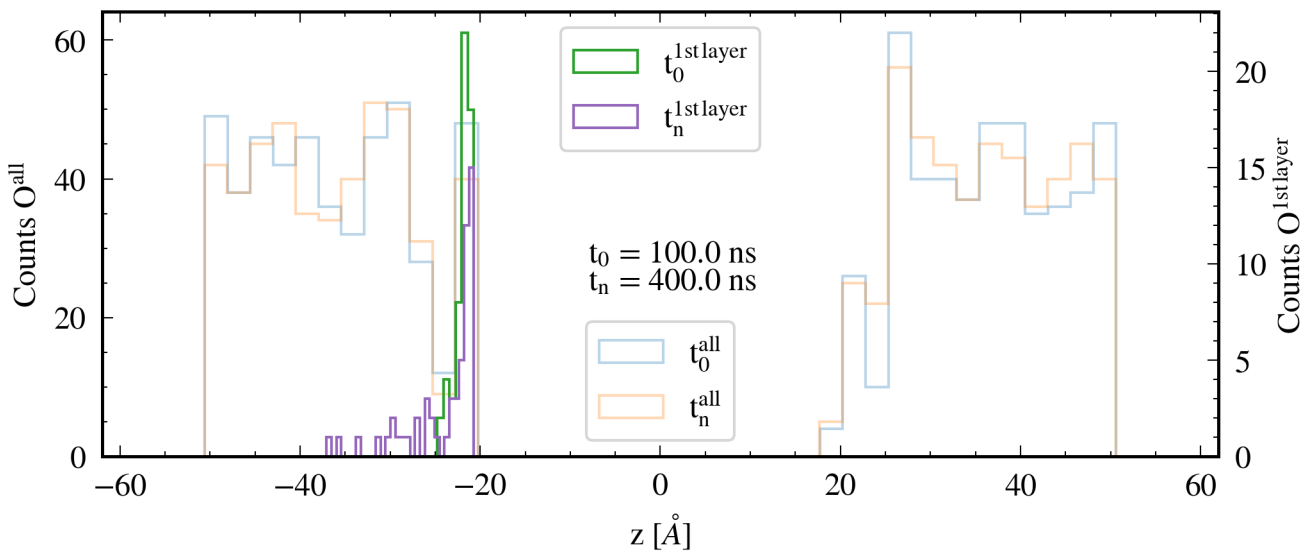


Figure S9: Histograms at 400 K at two different times (100 ns and 400 ns). First, the distribution of all  $O^{PEO}$  are shown at both times. Second, at 100 ns the LEFT  $O^{1st\ layer}$  are displayed (green histogram) as well as their positions at 400 ns (violet histogram).

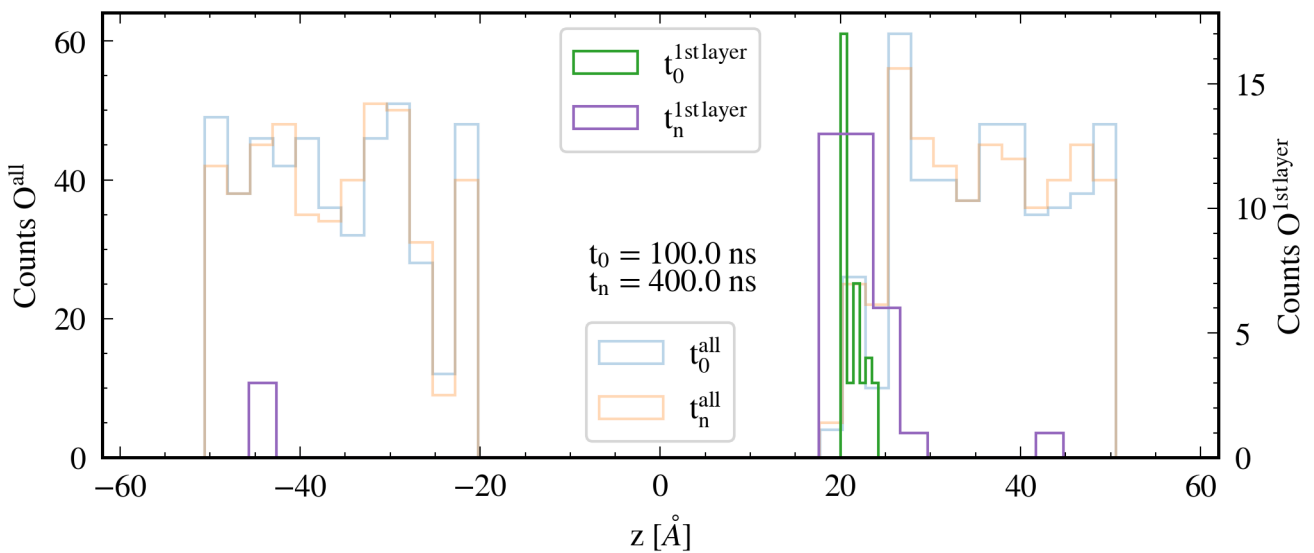


Figure S10: Histograms at 400 K at two different times (100 ns and 400 ns). First, the distribution of all  $O^{PEO}$  are shown at both times. Second, at 100 ns the RIGHT  $O^{1st\ layer}$  are displayed (green histogram) as well as their positions at 400 ns (violet histogram).

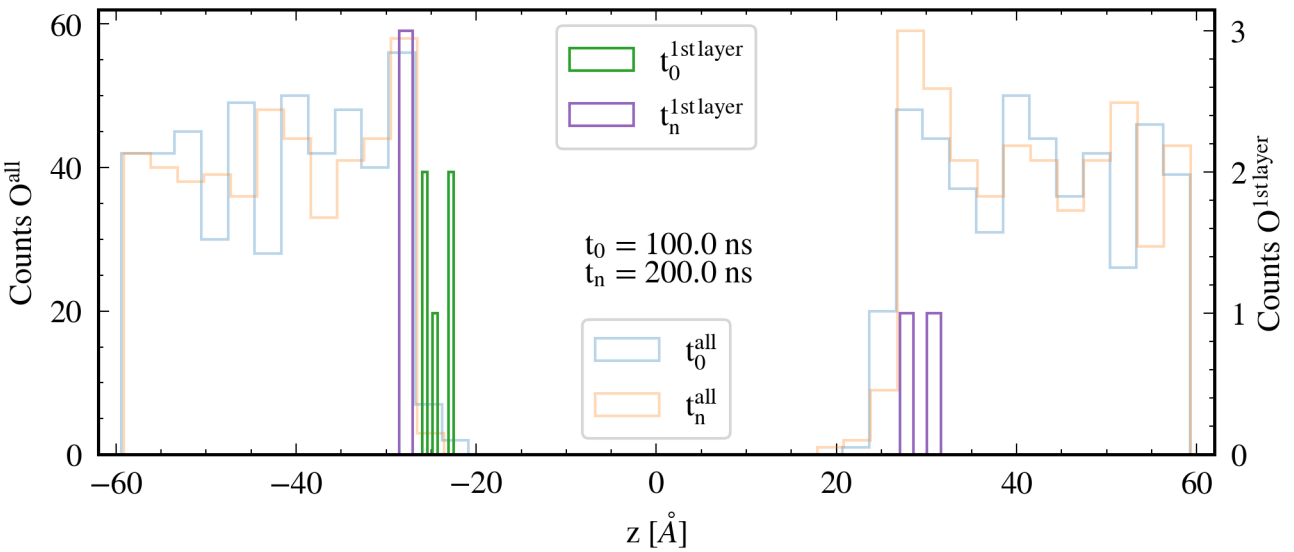


Figure S11: Histograms at 700 K at two different times (100 ns and 200 ns). First, the distribution of all  $O^{PEO}$  are shown at both times. Second, at 100 ns the LEFT  $O^{1st \, layer}$  are displayed (green histogram) as well as their positions at 200 ns (violet histogram).

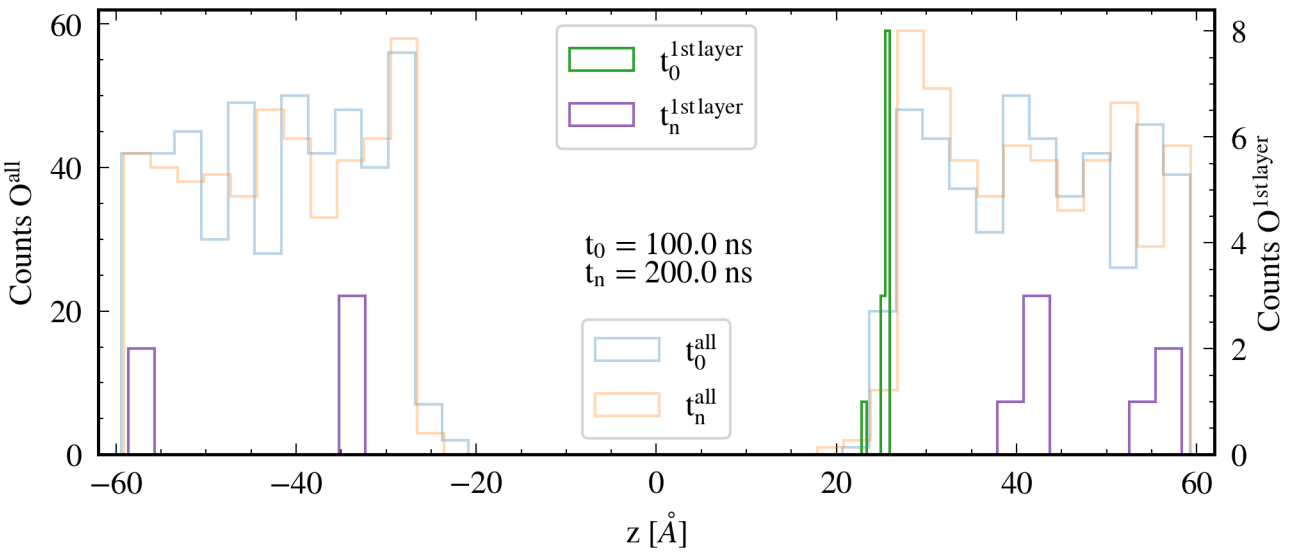
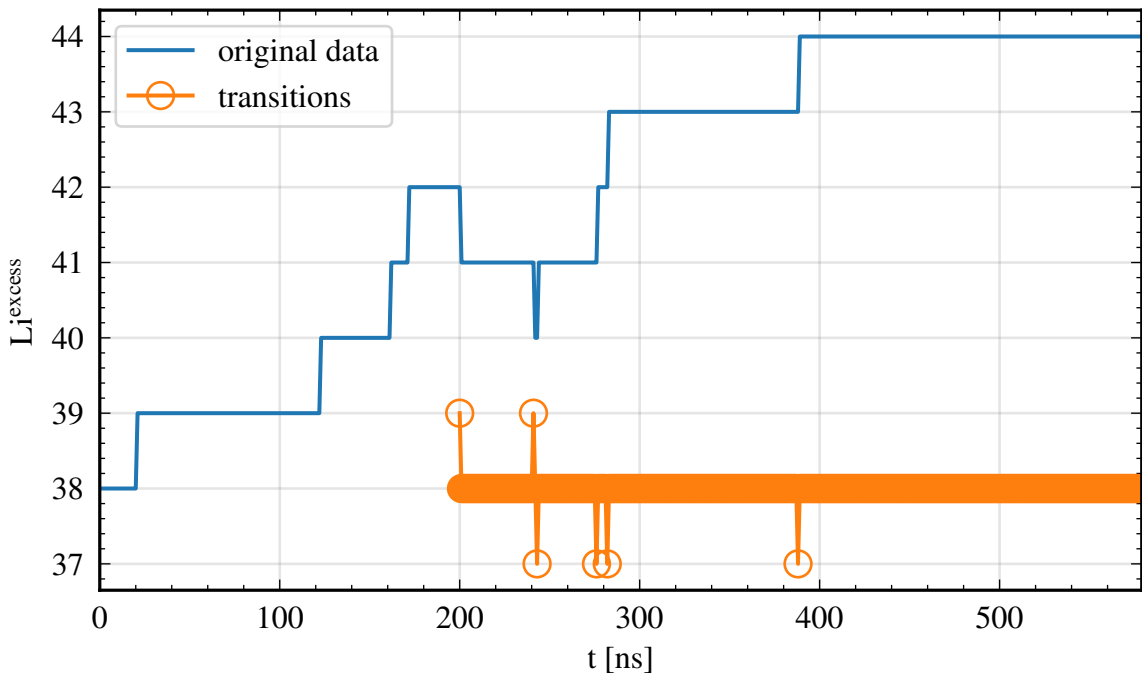
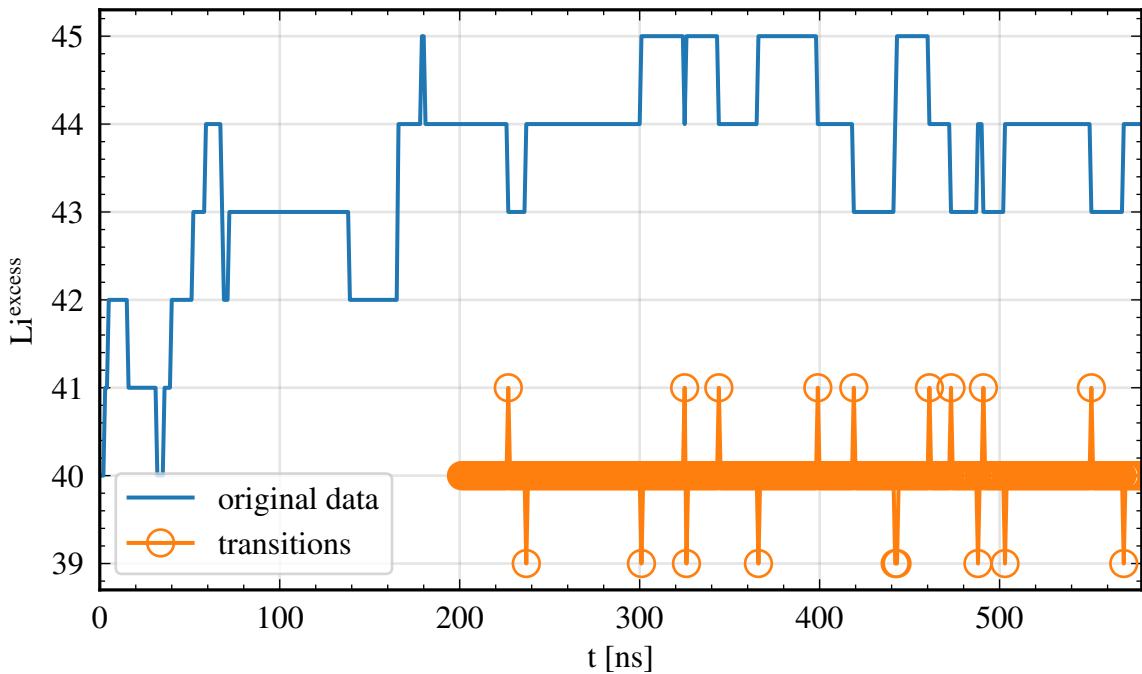


Figure S12: Histograms at 700 K at two different times (100 ns and 200 ns). First, the distribution of all  $O^{PEO}$  are shown at both times. Second, at 100 ns the RIGHT  $O^{1st \, layer}$  are displayed (green histogram) as well as their positions at 200 ns (violet histogram).

90LiTFSI-600K-Li

Figure S13:  $\text{Li}^+$  in and out LLZO region transitions at 600 K.

90LiTFSI-700K-Li

Figure S14:  $\text{Li}^+$  in and out LLZO region transitions at 700 K.

## Rationalization of the specific form of EC

To rationalize this approach we consider the situation of a symmetric two-state system (the states being denoted A and B) and consider a non-equilibrium (neq) population ( $3N$  particles in A,  $N$  particles in B) as well as an equilibrium (eq) population ( $N$  particles in A,  $N$  particles in B) with  $N$  much larger than one. From studying the binomial distribution for large  $N$  one can calculate the probabilities  $p_{neq}$  and  $p_{eq}$ , respectively, that after  $2k$  transitions one has exactly  $k$  transitions from A to B and  $k$  from B to A. One expects that this probability is smaller for the non-equilibrium case (denoted  $p_{neq}$ ) than for the equilibrium case (denoted  $p_{eq}$ ). A short calculation yields  $p_{neq}/p_{eq} = (3/4)^k$ . This implies that for larger values of  $k$  it becomes more and more

unlikely that a non-equilibrium initial condition gives rise to an equal number of transitions from A to B and vice versa. In an ad hoc manner, we choose  $p_{neq}/p_{eq} \approx e^{-1}$  as the limit where we use the observation of an equal number of transitions from A to B and from B to A, respectively, as an indicator of an equilibrium situation. Thus, the chosen functional form of EC should fulfill the condition that for an equal number of transitions it starts to be small for  $k \leq 4$  (no clear statement about initial equilibrium) and becomes larger for  $k > 4$  (stronger indication of initial equilibrium). Applying the functional form, suggested in this work, to the present example one obtains  $EC = 2k/(2k + \lambda)$ . Thus, the requirements are fulfilled if one chooses  $\lambda/2$  to be, e.g., 5, implying  $\lambda = 10$ . Naturally, in case of a different initial ratio this value would change (e.g. the transition value is 8 in case of a 2N:N distribution).